



Adsorption of naphthalene from vehicle-wash wastewater using eucalyptus wood waste derived biochar

Yu Shuang Ren^a, Muhammad Ilyas^{b,c,*}, Maooz Ahmad^d, Juma Muhammad^e, Muhammad Subhanullah^c, Ishaq Ahmad Mian^f

^aSchool of Economics and Management, Jilin Jianzhu University, Chang Chun 130117, China, email: rysmiracle@126.com (Y.S. Ren)

^bDepartment of Environmental Sciences, University of Peshawar, Peshawar, Khyber Pakhtunkhwa, Pakistan, Tel.: +923078064028; email: sirfilyas@yahoo.com (M. Ilyas)

^cDepartment of Environmental Sciences, Shaheed Benazir Bhutto University Wari Campus, Dir Upper, Khyber Pakhtunkhwa, Pakistan, email: subhanenv92@gmail.com (M. Subhanullah)

^dDepartment of Botany, Abdul Wali Khan University Mardan, Khyber Pakhtunkhwa, Pakistan, email: maoozahmadbd@gmail.com (M. Ahmad)

^eDepartment of Environmental Sciences, Shaheed Benazir Bhutto University Sheringal, Dir Upper, Khyber Pakhtunkhwa, Pakistan, email: juma@sbbu.edu.pk (J. Muhammad)

^fDepartment of Soil and Environmental Sciences, Agriculture University, Peshawar, Pakistan, email: ishaqmian@aup.edu.pk (I.A. Mian)

Received 30 April 2023; Accepted 10 August 2023

ABSTRACT

This article describes the production of eucalyptus wood waste biochar (EWB) and its use in the adsorptive removal of naphthalene (Nap) from vehicle wash wastewater (VWW). EWB was produced by carbonizing the waste eucalyptus wood at a high temperature in a nitrogen atmosphere. The produced EWB was chemically activated by being subjected to 1 M HCl in order to increase its effectiveness. The EWB was described using pertinent instrumental techniques such as surface area analysis, Fourier-transform infrared spectroscopy, and scanning electron microscopy. Nap adsorption from aqueous solutions through EWB was examined using batch adsorption tests. As adsorption parameters, initial EWB concentration, contact time, pH, temperature, and adsorbent dose were all examined. Under ideal conditions, the adsorption efficiency was computed and the Nap contents were determined using a UV spectrometer. The optimal conditions for the highest adsorption of Nap from VWW on the EWB adsorbents were found to be an initial concentration of 30 ppm, contact time of 90 min, temperature of 60°C, adsorbent dose of 0.30 g, and 5 pH. Kinetic and isotherm models were applied to evaluate the adsorbent capacity to bind Nap. The kinetic study shows that the adsorption of Nap onto EWB is controlled by pseudo-second-order kinetics. The results of the experiment demonstrated that the Langmuir isotherm model offered the best fit for the data. The values of thermodynamic parameters such as entropy (ΔS°), Gibb's free energy (ΔG°) and enthalpy (ΔH°) show that the adsorption process is spontaneous and exothermic in nature. The trial results revealed that the highest adsorption at optimum condition for Nap from VWW was 98.65% ($q_e = 141.52$ mg/g). The performances of certain commercial adsorbents utilized in practice were also compared with the results. This analysis showed that the new EWB has a significant potential (>95%) for removing and recovering Nap from industrial effluent.

Keywords: Biochar; Vehicle wash wastewater; Adsorptive removal; Naphthalene

* Corresponding author.

1. Introduction

Polycyclic aromatic hydrocarbons (PAHs) are recalcitrant and toxic organic pollutants, and consist of two or more fused benzene rings in linear, cluster or angular arrangements, and are associated with low water solubility [1]. Both natural and artificial sources release PAHs into the environment. Compared to anthropogenic sources in the environment, natural sources of PAHs are few [2]. Volcanic eruptions, oil seepages, thermal geological reactions, natural forest fires, prairie, and oil seepages are a few examples of natural sources [3]. Residential waste burning, agricultural processing, vehicle emissions, military operations, coal tar production, asphalt and shale oil production, coal conversion, metalworking, petroleum processing, steel and iron foundry works, aluminium smelting and coke production, and incomplete combustion are notable examples of the various anthropogenic sources responsible for the PAHs emissions [4]. Agricultural and medicinal products, resins, dyes, insecticides, and the production of pigments all frequently employ PAHs as lubricants [5]. The majority of the sources of PAHs in the aquatic system include polluted sediments, atmospheric deposition, and unintentional leakage. PAHs are prevalent in tar deposits, coal, and oil [6].

High molecular weight PAHs, which contain 6, 5, or 4 benzene rings, and low molecular weight PAHs, which contain 3 or 2 benzene rings, can be divided into two main classes [7]. PAHs are a major problem in the aquatic system due to their mutagenic and carcinogenic properties, high lipophilicity, persistence, and dangerous nature [8]. The carcinogenicity of PAHs typically rises with increasing molecular weight. Both long-term and short-term health effects can be caused by PAHs, with the former including asthma symptoms, breathing problems, lung abnormalities, liver and kidney damage, cataracts, and immune system suppression [5]. Although the short-term health consequences of PAHs on people are unclear, occupational exposure to high levels of PAHs may cause temporary side effects like diarrhoea, eye irritation, vomiting, disorientation, and nausea [5]. Many PAHs have been discovered to exist in the tissues of both plants and animals, in water bodies, in soil and sediments, and in the air, indicating their presence in the environment [9]. Since PAHs are persistent and non-biodegradable, they enter the food chain through the soil and move to the human body by skin contact, inhalation, or ingestion [5].

Several techniques are being developed over time to remove PAHs from contaminated soil and water, in an effort to lessen the potential risk to human health and the environment. Biological, thermal, chemical, and physical processes, as well as phytoremediation (including phytodegradation, phytostabilisation, phytoextraction, rhizofiltration, bioaugmentation, biostimulation, natural attenuation, chemical precipitation, electrolysis, adsorption, photolysis, ion exchange, oxidation, radio frequency heating, thermal desorption, and incineration methods) are the main treatment techniques for PAHs contaminated water, sediment, as well as soil [9]. However, the majority of these techniques have some challenges, such as difficult operational processes, high maintenance expenses, and high investment prices. Moreover, several of these treatment methods produce

secondary byproducts, some of which are carcinogenic and mutagenic (e.g., trihalomethanes, haloacetic acid), which worsens the effects on public health [10,11].

The adsorption approach has a straightforward design, is simple to use, is unaffected by harmful contaminants, and is inexpensive. As a result, the method to remove PAHs from aqueous media is effective. The adsorption approach can achieve an eradication effectiveness of 99.9% [12]. In this way, people are becoming more and more eager to discover practical adsorbents to remove harmful pollutants from water. Pollutants will gather on the adsorbent's surface or contact during the adsorption process. Adsorption takes place at the point when the solid adsorbent and sewage meet during the water treatment process. Adsorbent and adsorbate are the names for the adsorption phase and the contaminants that are adsorbed, respectively [12]. Among the many adsorbents employed for this are hen feathers [13], waste polyethylene terephthalate/biochar/bentonite and waste polystyrene/biochar/bentonite [14,15], activated carbon [9], montmorillonite clay [16], waste rubber tires [17], papaya peel carbon [18], chitosan grafted polyaniline [19], various materials as biosorbents [20], mixed biosorbents (custard apple seeds and *Aspergillus niger*) [21], immobilized fungal biomass [22], mixed biosorbent of agro waste and bacterial biomass [23], mixed biomass [*Aspergillus campestris* and two forms of *Delonix regia* seed (raw and acid treated *Delonix regia* seed)] [24] and nano alumina [25].

In the present investigation, the EWB has been prepared successfully by a simple and low-cost method. Investigations were conducted on the structural characteristics of the EWB as well as the adsorption states of naphthalene (Nap). Through batch studies, the effectiveness of EWB adsorption was assessed, and its adsorption behaviour for Nap was carefully examined, including the effect of initial Nap concentration, temperature, contact time, pH, adsorbent dose, adsorption isotherm, and adsorption kinetics. This study makes a significant contribution to the removal of hazardous Nap from wastewater and establishes a new benchmark for lowering environmental pollution by reducing solid waste. This in turn raises the local environment aesthetic value.

2. Materials and methods

In the current study, waste eucalyptus wood was converted into biochar, which was then used as an adsorbent to remove Nap from vehicle wash wastewater (VWW). In order to achieve the above objectives, the following methods were adopted.

2.1. Sample collection

In 2.5 L amber glass bottles that had already been cleaned, VWW samples were collected. The University of Agriculture (Peshawar, Pakistan) provided EWB made from eucalyptus wood waste.

2.2. Synthesis of biochar from eucalyptus wood waste

Waste eucalyptus wood samples were cleaned, dried and chopped into small pieces. Waste eucalyptus samples were converted to EWB by carbonization at high temperature

under an inert atmosphere in a specially designed steel reactor. About 5 g of waste eucalyptus wood was taken into a steel reactor and inserted into a tube furnace, a nitrogen supply was connected to the reactor and heated to 450°C for 1 h. The carbonaceous residue was ground into powder, then passed through a 100-mesh sieve, and stored in glass vials for further study.

2.3. Characterization of EWB

Scanning electron microscopy (SEM), Fourier-transform infrared spectroscopy (FTIR), and surface area were used to characterize the EWB that was synthesized in the laboratory. Using a scanning electron microscope made by JEOL (Tokyo, Japan), the surface morphology of the EWB was investigated. A Nicolet iS10 FTIR spectrometer (Cary 630, Agilent Technologies, USA) with a scanning range of 4,000–400 cm⁻¹ was used to measure the FTIR spectra. The average pore size, total pore volume, and specific surface area were calculated using a Quantachrome, USA, Model NOVA 2200e porosimetry system and surface area.

2.4. Adsorption experiments

Batch mode adsorption studies were used to study the adsorption of Nap from VWW over EWB. EWB dosage 0.1, 0.2, 0.3, and 0.4 g, contact time 15, 30, 45, 60, 90, and 120 min, pH 1–7, and Nap concentrations 10, 20, 30, and 40 ppm were some of the factors that were examined in the study. The total volume of samples used for the experiment was 100 mL. All Nap adsorption and kinetic models were run in a batch setup with 500 mL Erlenmeyer flasks at various temperatures. At different temperatures (30°C, 40°C, 50°C, and 60°C), the samples were stirred at 150 rpm in a magnetic stirrer until equilibrium was attained. Only the average values of the three triplicates are shown for all tests.

2.5. Analyses and calculations

According to Table 1, the equilibrium concentration, q_e (mg/g) and % q_e were computed.

The numerical models shown in Tables 2 and 3 were used to fit the data [14,15]. The Nap concentrations in the solution were measured using Shimadzu UV-1700 UV-Vis spectrophotometry (Germany) (200–270 nm).

Table 1
Equations used for q_e and % q_e calculations

	Equation
Equilibrium concentration	$q_e = \frac{[(C_0 - C_i)V]}{M} \quad (1)$ <p>where, C_0 (mg/L) = Initial Nap concentration; C_i (mg/L) = Equilibrium Nap concentration; V (L) = Volume of solution; M (g) = Mass of EWB.</p>
Percentage removal	$\%q_e = \frac{[(C_0 - C_i) \times 100]}{C_0} \quad (2)$

The effect of temperature on the thermodynamics variables ΔG° , ΔH° , and ΔS° was also examined (Table 4) [14,15].

3. Results and discussion

3.1. Characterization of EWB

SEM, FTIR, and surface area analysis were used in the laboratory to examine the characteristics of biochar produced

Table 2
Isotherm models used in the study

Model	Equation
Langmuir	$\frac{C_e}{q_e} = \frac{1}{KQ_{\max}} + \frac{C_e}{Q_{\max}} \quad (3)$ <p>Since, q_e is the quantity of adsorbed Nap on the EWB at equilibrium (mg/g) and C_e is the equilibrium-concentration of the Nap (mg/L)</p>
Freundlich	$\ln q_e = \ln K_f + \frac{1}{n} \ln C_e \quad (4)$ <p>Since: n and K_f are the adsorption intensity and capability, respectively</p>

Table 3
Kinetic models used in the study

Model	Equation
Pseudo-first-order	$\ln(q_e - q_t) = \ln q_e - k_1 t \quad (5)$ <p>Since: q_e and q_t are the amounts of adsorbed Nap (mg/g) at equilibrium and time t (min), respectively, and k_1 is the rate-constant of pseudo-first-order (min⁻¹)</p>
Pseudo-second-order	$\frac{t}{q_t} = \frac{t}{q_e} + \frac{1}{k_2 q_e^2} \quad (6)$ <p>Since: k_2 is the rate-constant of pseudo-second-order adsorption (g/mg·min) and at equilibrium the sorption capacity is presented by q_e</p>

Table 4
Equations used for the thermodynamic parameters calculations

Gibb's free energy	$\Delta G^\circ = -RT \ln K_D \quad (7)$ <p>where R is the ideal gas constant, 8.314 J/K·mol; T is the absolute temperature in K; K_D is the equilibrium coefficient of the PAHs adsorption on the EWB</p>
Enthalpy	$\Delta H^\circ = R \frac{T_2 T_1}{T_2 - T_1} \ln \frac{k_2}{k_1} \quad (8)$
Entropy	$\Delta S^\circ = \frac{\Delta H^\circ - \Delta G^\circ}{T} \quad (9)$

from eucalyptus wood waste. The surface morphology of dry biomass (Fig. 1a) depicts a mesoporous structure, with some extraneous particles spread on the surface. The particle morphology in the SEM micrograph of EWB (Fig. 1b) was irregular. Uniquely sized lumps and particles smaller than 5 microns in size and up to 30 microns in size make up EWB. After adsorbing Nap, the EWB surface appears shiny, smooth, and has a closed pore structure in Fig. 1c. This change may be the result of a physicochemical interaction between the functional groups on the EWB surface and Nap.

The EWB synthesized from eucalyptus wood waste was characterized by FTIR spectroscopy. The FTIR spectrum of EWB is shown in Fig. 2a, which shows a distinct peak at 3,000 and 2,800 cm^{-1} , corresponding to aromatic C–H and methylene C–H bonds. The peaks at 1,630 cm^{-1} indicates C=C stretching vibrations, whereas the peak positioned at 1,500 cm^{-1} exhibits the C=C groups for aromatics, that is, SP^2 hybridized carbon. The bands positioned at 1,447 cm^{-1} can be assigned to methylene CH_2 configuration. The peak positioned at 693 cm^{-1} arising from C–H bending vibration. The EWB FTIR spectrum after desorption is shown in Fig. 2b. The absorption bands were detected at 2,919 cm^{-1} ($=\text{CH}_2$, stretching), 1,599 cm^{-1} (C=C, stretching), 1,493 cm^{-1} (C=C, stretching), 1,451 cm^{-1} (CH_2 stretching), 1,013 cm^{-1} (C–O, stretching), 698 cm^{-1} (C–H, stretching) and 521 cm^{-1} (C–H, stretching). The point of zero charge (PZC) was found

to be 4.25 (Fig. 3) and its surface will be negatively and positively charged at the pH above and below PZC.

The N_2 adsorption isotherms at 77.35 K were used to derive the surface area parameters for EWB (Fig. 4). The outcomes are displayed in Table 5. According to the surface analysis findings (Table 5), the calculated S_{BJH} for EWB was 14.10 m^2/g . The S_{BET} was found to be 18.37 m^2/g , with pore volume of 0.01 cm^3/g and a pore radius of 14.90 Å. The statistics demonstrate that the EWB adsorbent has a large pore size and a high surface area. Therefore, EWB has better adsorption potential. The surface characteristics were seen to decrease after adsorption, which confirmed the adsorption of Nap.

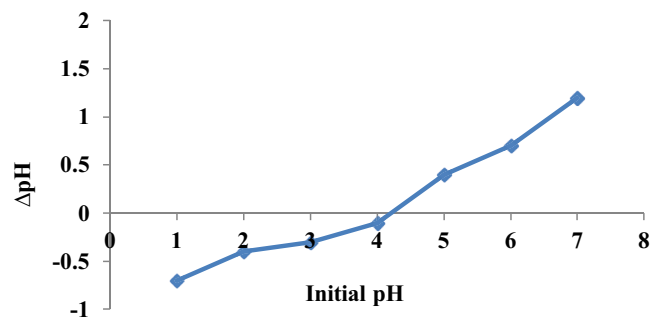


Fig. 3. Determination of point of zero charge of EWB.

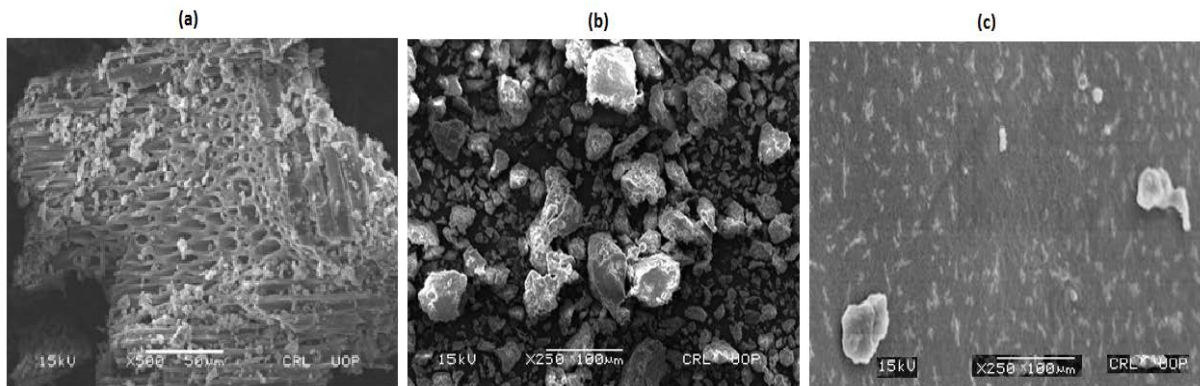


Fig. 1. Scanning electron microscopy images of dry biomass (a), EWB before Nap adsorption (b), and EWB after Nap adsorption (c).

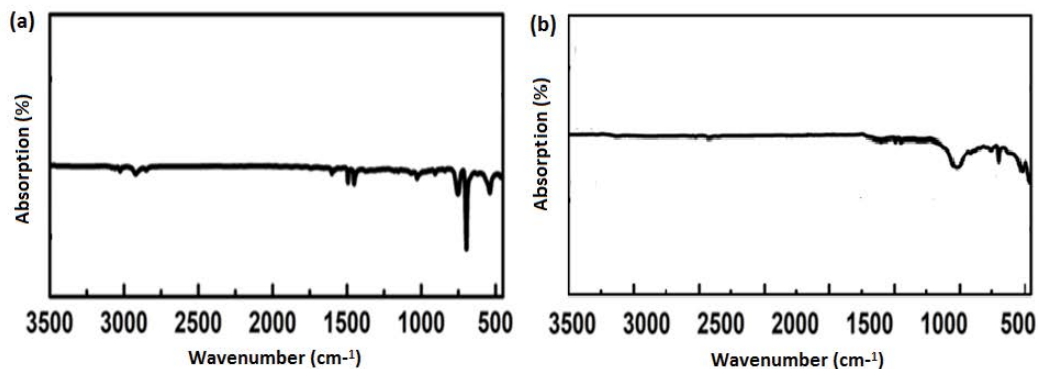


Fig. 2. Fourier-transform infrared spectra of EWB before adsorption (a) and after desorption (b).

3.2. Investigation of the adsorption parameters

To find the optimal conditions required for maximum Nap adsorption, adsorption was investigated under various Nap concentrations, adsorbent doses, temperature, pH levels, and contact time.

3.2.1. Effect of contact time

Using a series of adsorption studies at various periods, ranging from 15–120 min, the effects of adsorption time on the removal of Nap from VWW were examined. According to the findings in Fig. 5, Nap adsorption rises with increasing contact time and reaches its maximum in 90 min. There may be active adsorption sites, which could help to explain this pattern. The number of active sites that are initially available for adsorption on the adsorbent surface rapidly decreases as adsorption proceeds. Once all active surfaces have been covered, which takes 90 min [26], the adsorption is complete. In earlier studies on the adsorption of toxicants by various adsorbents, similar results were also reported, that is, the adsorption increased with the increase of the adsorption period and approached equilibrium ($q_e = 141.52$ mg/g) [27,28].

3.2.2. Effect of temperature

Fig. 6 illustrates the adsorption of Nap from VWW at various temperatures, ranging from 30°C to 60°C. Findings indicate that Nap adsorption rises with temperature and reaches a maximum at 60°C. However, when the temperature rises more, the percentage of Nap adsorption decreases. The weak Van der Waals forces involved in physical adsorption weaken at high temperatures, which cause a decrease in the rate of adsorption, but at temperatures above the optimum, the adsorption slows down. The

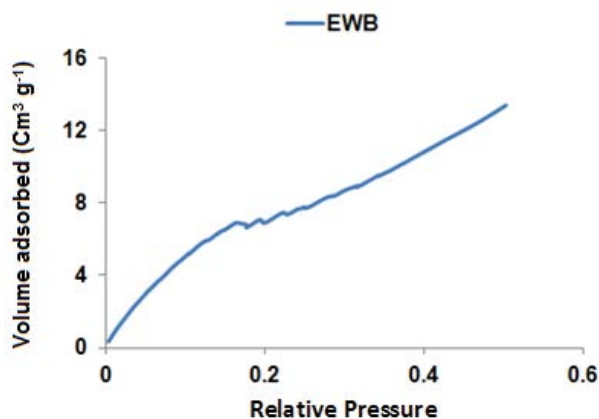


Fig. 4. N₂ adsorption isotherms of EWB at 77 K.

Table 5
Surface properties of the EWB

Adsorbent	S_{BJH} (m ² /g)	S_{BET} (m ² /g)	Pore radius (Å)	Pore volume (cm ³ /g)
EWB (before adsorption)	14.10	18.37	14.90	0.01
EWB (after adsorption)	1.80	1.92	2.36	0.0001

concentration is expected to increase as the temperature rises since physical adsorption is often exothermic in nature [29]. On the other hand, because the chemical adsorption is endothermic, the rate of adsorption increases as the temperature does [30]. The percentage of Nap adsorbed in the current situation rises with temperature and reaches a maximum at 60°C before falling off again as the temperature rises. Furthermore, increasing temperature indicated an increased likelihood of adsorption at higher temperatures, which is consistent with previous findings [27,28].

3.2.3. Effect of adsorbent dose

For 30 mL of VWW, batch adsorption studies were conducted with EWB dosages ranging from 0.1 to 0.4 g. Fig. 7 presents the findings. The results show that the adsorption of Nap increased linearly as the adsorbent dosage increased, with the highest adsorption of Nap being achieved at a dose of 0.3 g of adsorbent per 30 mL of VWW. As more and more

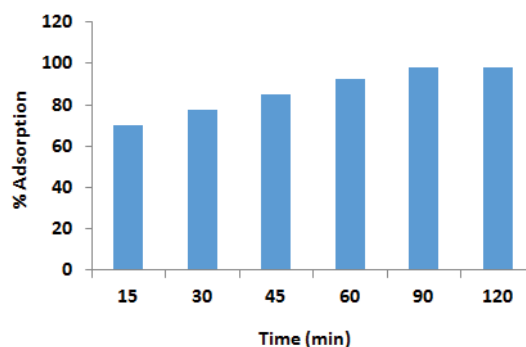


Fig. 5. Effect of contact time on the % adsorption of Nap over the EWB.

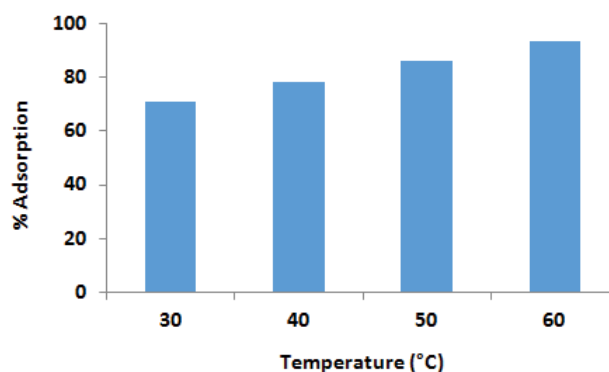


Fig. 6. Effect of temperature on the % adsorption of Nap over the EWB.

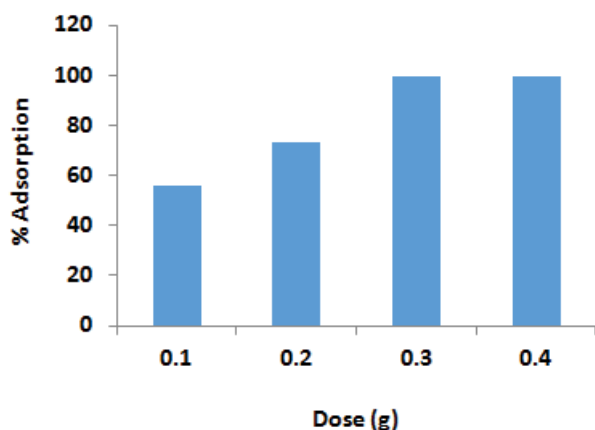


Fig. 7. Effect of adsorbent dose on the % adsorption of Nap over the EWB.

adsorbent is added, the number of active adsorbent sites increases, which is likely the cause of the increased adsorption of Nap with the rise in adsorbent dose. The adsorption of Nap, however, decreases with subsequent adsorbent dose increases because excess EWB aggregates and reduces the number of active sites on the surface that are available for adsorption [31]. The ideal dose of 0.3 g of EWB for 30 mL of VWW was chosen based on the largest amount of Nap adsorbed.

3.2.4. Effect of initial concentrations

The adsorption of Nap by EWB was investigated at varied initial Nap concentrations. The data are shown in Fig. 8. This suggests that as the initial Nap concentration increases from 10 to 40 mg/L, the rate of Nap adsorption on EWB increases. When the initial Nap concentration is raised, Nap binds to the surface-active sites of EWB, causing this. A more grounded primary impetus is created when the concentration of Nap grows due to the presence of a significant concentration gradient, which exploits active sites to increase the amount of EWB that can be absorbed per unit mass while overcoming the mass exchange resistance [15].

3.2.5. Effect of pH

The adsorption of adsorbates onto the charged adsorbents is significantly influenced by the pH of the medium. The effect of pH on the adsorption of Nap utilising EWB was investigated in the current study in the range of 1–7 (Fig. 9). The initial pH values of the Nap mixture solutions were altered at 1, 2, 3, 4, 5, 6, and 7 by a few drops of diluted 0.1 M NaOH or HCl solution. The results of the study showed that the adsorption process is highly pH dependent, and increasing the pH from 1 to 5 increased the adsorption of Nap. However, adsorption decreases if the pH is increased, so pH 5 was chosen for further study. EWB has a PZC value of 4.25, indicating that its surface is positively and negatively charged at pH values below and above the PZC, respectively. The data showed that there was no significant difference in the adsorption of Nap

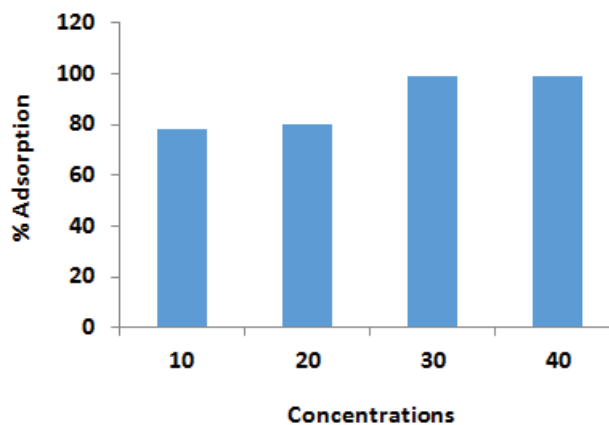


Fig. 8. Effect of initial concentrations on the % adsorption of Nap over the EWB.

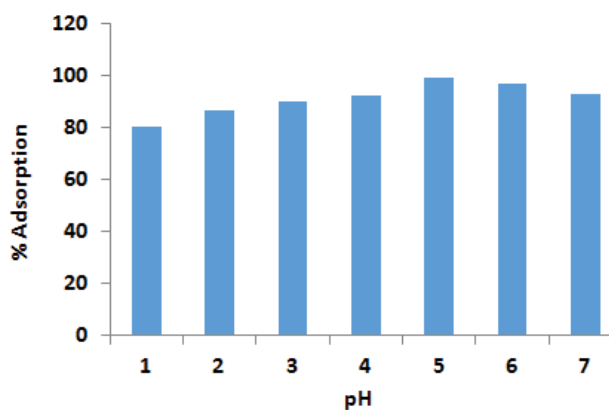


Fig. 9. Effect of adsorbent dose on the % adsorption of Nap over the EWB.

in the pH range from 1 to 4, which may be because there are too many H^+ ions competing for the same adsorption sites as Nap. The adsorption capacity increases at pH 4 and reaches a maximum at pH 5. Similar results have been observed by researchers using various adsorbents to adsorb PAHs [9,27].

3.3. Adsorption kinetics

To analyse the adsorption kinetics, the adsorption data was interpreted using pseudo-first-order and pseudo-second-order kinetics models. The pseudo-first-order and pseudo-second-order kinetic graphs are shown in Fig. 10a and b, the predicted kinetic parameters are shown in Table 6. In spite of the fact that the correlation factor R^2 (0.991) for the pseudo-second-order model was the highest, showing that the adsorption system follows a pseudo-second-order kinetics. According to the pseudo-second-order model [15], it is generally assumed that the adsorption of Nap onto EWB is a chemisorption in which valence forces are generated through the contribution or exchange of electrons between the adsorbent and the adsorbate.

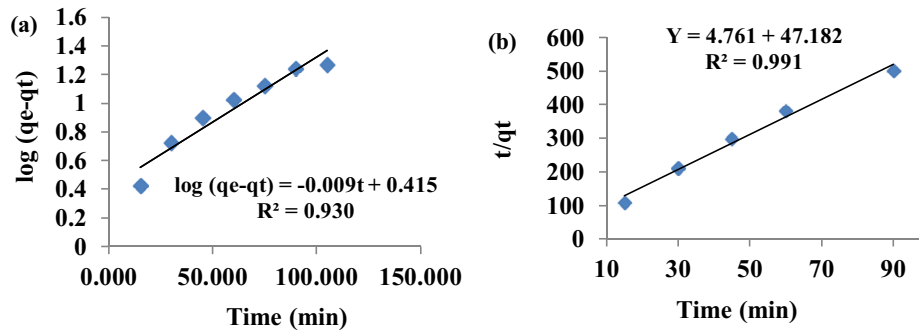


Fig. 10. Pseudo-first-order (a) and pseudo-second-order (b) kinetics for the adsorption of Nap onto EWB.

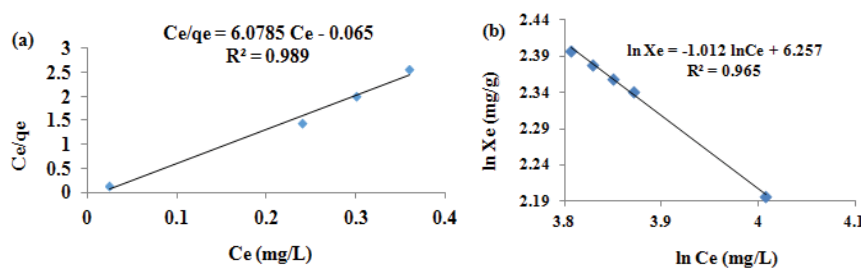


Fig. 11. Langmuir (a) and Freundlich (b) isotherms for the adsorption of Nap onto EWB.

Table 6
Kinetic parameters of Nap adsorption over EWB

	Pseudo-first-order equation parameters	Pseudo-second-order equation parameters	
k_1 (min^{-1})	0.021	K_2 (mg/g·min)	0.001
q_e (mg/g)	2.600	q_e (mg/g)	0.210
R^2	0.930	R^2	0.991

Table 7
Nap adsorption isotherm parameters with their corresponding correlation coefficients

	Langmuir isotherm parameters	Freundlich isotherm parameters	
q_m (mg/g)	0.164	N	0.988
k_1	0.395	K_f	1.834
R^2	0.989	R^2	0.965

3.4. Adsorption equilibrium study

To examine the nature and viability of the adsorption of the adsorbate over the adsorbent, the adsorption data was fitted into the Langmuir and Freundlich adsorption isotherms. The Langmuir isotherm explains the adsorption as the formation of a monolayer of adsorbate on the adsorbent surface. Fig. 11a and b display the Langmuir and Freundlich adsorption isotherm plot, and Table 7 provides a comprehensive list of isotherm features. The fact that the Nap adsorption data gave a superior match in the Langmuir isotherm model is shown by the greater estimation of correlation coefficient for Langmuir than for Freundlich isotherm. Langmuir isotherm describes the adsorption by the formation of a monolayer of adsorbate on the adsorbent surface. Adsorbate is not moved over the adsorbent; instead, it is adsorbed at fixed adsorptive sites [9].

3.5. Thermodynamic study

The nature of adsorption was further studied through the evaluation of several thermodynamic parameters. The values of ΔG° , ΔH° , and ΔS° for the adsorption of Nap

Table 8
Thermodynamic parameters of EWB at different temperatures

Temperature (K)	Nap		
	ΔG° (kJ/mol)	ΔH° (kJ/mol)	ΔS° (J/K·mol)
293	-8.05		
313	-5.61		
333	-4.96	-38.53	-102.82
353	-2.89397		

over EWB formed from eucalyptus wood waste are shown in Table 8. Due to the fact that the adsorption process is spontaneous when ΔG° is negative (-ve) and non-spontaneous when it is positive (+ve). It is clear that the adsorption is spontaneous in nature because the ΔG° result in this situation is negative. Furthermore, as the temperature rises, the ΔG° value becomes more negative. The negative finding for ΔH° , however, indicates that the adsorption process is exothermic. The high value of ΔS° , on the other

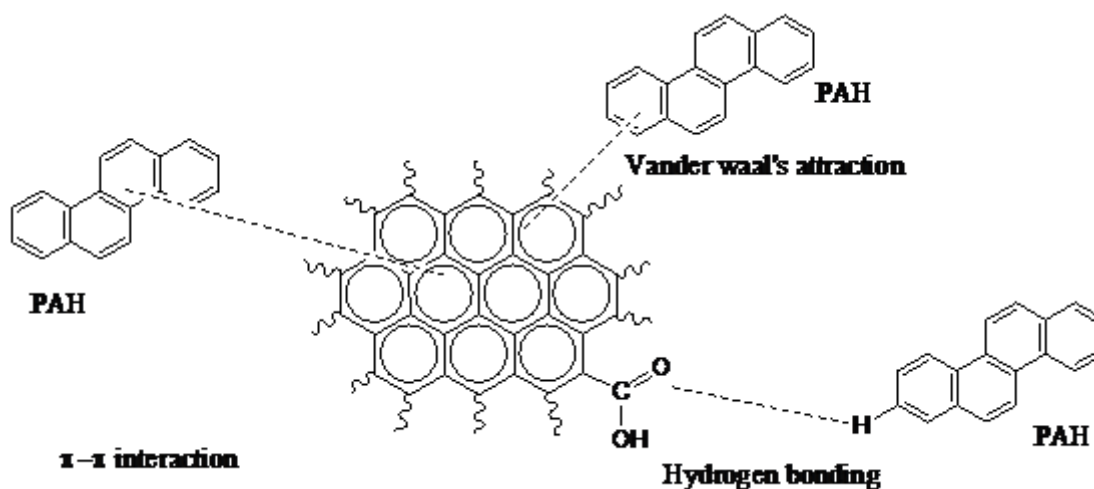


Fig. 12. Mechanism of Nap adsorption onto EWB.

Table 9
Comparison of different adsorbents used for Nap adsorption

Materials	PAHs removal efficiency (%)	References
Clinoptilolite	Nap (100)	[33]
Activated carbon bed	Nap (98.1)	[34]
Activated carbon	Nap (97)	[35]
Coke-derived porous carbon	Nap (>99 for all PAHs)	[36]
EWB	Nap (98.65)	This article

hand, denotes a spontaneous adsorption process in which randomness increases. These findings concur with those presented in the literature [9].

3.6. Mechanisms of Nap adsorption

According to the parameters of the solution, the adsorbent surface properties, and the kind of the adsorbate, biochar typically absorbs contaminants from aqueous solutions. There have been several proposed methods by which the functional groups on the carbon surface may influence the adsorption process from aqueous solution: hydrogen bonding, interaction of electron donors and acceptors as well as π - π dispersive interactions [9]. According to Lyklema [32], the process used to adsorb PAHs from aqueous solution is essentially an exchange one. Because of this, it has been suggested that the adsorption of organic compounds on the surface of EWB involves a complex interaction between electrostatic and dispersion interactions, particularly in the case of weak organic electrolytes. However, because Nap are not thought to be electrolytic, van der Waals dispersive interactions and intermediate hydrogen bonding have emerged as the two primary mechanisms put forth in the literature. The mechanism of adsorption of Nap by EWB is given in Fig. 12.

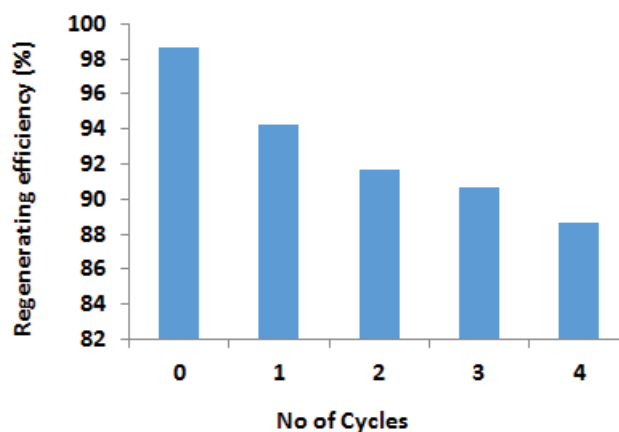


Fig. 13. Regenerating efficiency of EWB.

3.7. Comparison of adsorption potential of different adsorbents

Table 9 provides a comparison of the adsorption performance of the various adsorption media published in the literature and the EWB, for the adsorption of Nap. The choice of adsorbent for water treatment applications depends on a variety of parameters, including efficiency, nontoxicity, availability of material, reusability, and flexibility. With an adsorption effectiveness of >95% for Nap, EWB demonstrates considerable promise for applications in water treatment.

3.8. Desorption and reusability

Desorption and regeneration of adsorbents are crucial components of adsorption processes because they govern the economics of water treatment technology. In this study, deionized water and 0.1 M HCl was used for the desorption experiment. The spent EWB was added to 0.1 M HCl and was agitated for 30 min, the EWB was then recovered by filtration followed by drying in oven. The dried, cleaned EWB was then used to absorb a new batch of wastewater.

EWB may be reused, according to regeneration studies that were conducted in batches using 100 mL of VWW (Fig. 13).

4. Conclusion

Herein, we provide a simple method for the preparation of EWB from eucalyptus wood waste. The prepared EWB can be severed as an efficient adsorbent to remove Nap from VWW (>95%). The large specific surface area of EWB provides sufficient active adsorption sites for Nap. In addition, a thorough investigation of the external factors affecting the adsorption performance was also carried out. The results showed that EWB had high removal efficiency and enhanced reusability. The result shows that EWB has the highest removal efficiency of Nap from VWW (>95%). The outcomes demonstrate that the pseudo-second-order rate equation may accurately replicate the rate of Nap adsorption by EWB. The experimental results and the Langmuir isotherm model correlate well, pointing to a monolayer adsorption mechanism. The values of thermodynamic parameters such as ΔS° , ΔG° and ΔH° show that the adsorption process is spontaneous and exothermic in nature. The results of this study demonstrate the potential of EWB as a potential adsorbent to efficiently adsorb Nap from VWW. The current research demonstrates to be a milestone in the reduction of environmental pollution as far as wastewater reduction is concerned. In future work, we plan to examine the adsorption efficiency of EWB for various organic and inorganic pollutants.

Research funding

The authors acknowledge the funding offered by University of Peshawar, Khyber Pakhtunkhwa, Pakistan.

Conflict of interest

Authors state no conflict of interest.

Informed consent

Informed consent is not applicable.

Ethical approval

The conducted research is not related to either human or animal use.

References

- [1] A.R. Johnsen, U. Karlson, PAH degradation capacity of soil microbial communities—does it depend on PAH exposure?, *Microb. Ecol.*, 50 (2005) 488–495.
- [2] M. Charlesworth, M. Service, C.E. Gibson, PAH contamination of western Irish Sea sediments, *Mar. Pollut. Bull.*, 44 (2002) 1421–1426.
- [3] Z. Qamar, S. Khan, A. Khan, M. Aamir, J. Nawab, M. Waqas, Appraisal, source apportionment and health risk of polycyclic aromatic hydrocarbons (PAHs) in vehicle-wash wastewater, Pakistan, *Sci. Total Environ.*, 605 (2017) 106–113.
- [4] S. Hall, R. Tang, J. Baeyens, R. Dewil, Removing polycyclic aromatic hydrocarbons from water by adsorption on silicagel, *Polycyclic Aromat. Compd.*, 29 (2009) 160–183.
- [5] H.I. Abdel-Shafy, M.S.M. Mansour, A review on polycyclic aromatic hydrocarbons: source, environmental impact, effect on human health and remediation, *Egypt. J. Pet.*, 25 (2016) 107–123.
- [6] M. Blanchard, M.J. Teil, D. Ollivon, L. Legenti, M. Chevreuil, Polycyclic aromatic hydrocarbons and polychlorobiphenyls in wastewaters and sewage sludges from the Paris area (France), *Environ. Res.*, 95 (2004) 184–197.
- [7] M. Waqas, S. Khan, C. Chao, I. Shamshad, Z. Qamar, K. Khan, Quantification of PAHs and health risk via ingestion of vegetable in Khyber Pakhtunkhwa Province, Pakistan, *Sci. Total Environ.*, 497 (2014) 448–458.
- [8] A.J. Sweetman, K.C. Jones, Declining PCB concentrations in the UK atmosphere: evidence and possible causes, *Environ. Sci. Technol.*, 34 (2000) 863–869.
- [9] M. Ilyas, W. Ahmad, H. Khan, Utilization of activated carbon derived from waste plastic for decontamination of polycyclic aromatic hydrocarbons laden wastewater, *Water Sci. Technol.*, 84 (2021) 609–631.
- [10] I. Oller, S. Malato, J. Sánchez-Pérez, Combination of advanced oxidation processes and biological treatments for wastewater decontamination—a review, *Sci. Total Environ.*, 409 (2011) 4141–4166.
- [11] C. Comninellis, A. Kapalka, S. Malato, S.A. Parsons, I. Poullos, D. Mantzavinos, Advanced oxidation processes for water treatment: advances and trends for R&D, *J. Chem. Technol. Biotechnol.*, 83 (2008) 769–776.
- [12] I. Ali, Mohd. Asim, T.A. Khan, Low-cost adsorbents for the removal of organic pollutants from wastewater, *J. Environ. Manage.*, 113 (2012) 170–183.
- [13] J. Mittal, A. Mittal, Hen Feather: A Remarkable Adsorbent for Dye Removal, S.K. Sharma FRSC, Ed., *Green Chemistry for Dyes Removal from Wastewater: Research Trends and Applications*, Scrivener Publishing LLC, USA, 2015, pp. 409–457.
- [14] M. Ilyas, W. Ahmad, H. Khan, S. Yousaf, Potentially poisonous elements removal from vehicle-wash wastewater and aqueous solutions using composite adsorbents, *Desal. Water Treat.*, 224 (2021) 331–342.
- [15] M. Ilyas, W. Ahmad, H. Khan, I. Ahmad, Application of composite adsorbents prepared from waste PS and PET for removal of Cr and Cu ions from wastewater, *Desal. Water Treat.*, 171 (2019) 144–157.
- [16] N.M. Alandis, W. Mekhamer, O. Aldayel, J.A.A. Hefne, M. Alam, Adsorptive applications of montmorillonite clay for the removal of Ag(I) and Cu(II) from aqueous medium, *J. Chem.*, 2019 (2019) 7129014, doi: 10.1155/2019/7129014.
- [17] H. Daraei, A. Mittal, Investigation of adsorption performance of activated carbon prepared from waste tire for the removal of methylene blue dye from wastewater, *Desal. Water Treat.*, 90 (2017) 294–298.
- [18] R. Ahmad, I. Hasan, A. Mittal, Adsorption of Cr(VI) and Cd(II) on chitosan grafted polyaniline-OMMT nanocomposite: isotherms, kinetics and thermodynamics studies, *Desal. Water Treat.*, 58 (2017) 144–153.
- [19] J. Mittal, R. Ahmad, A. Mariyam, V.K. Gupta, A. Mittal, Expedient and enhanced sequestration of heavy metal ions from aqueous environment by papaya peel carbon: a green and low-cost adsorbent, *Desal. Water Treat.*, 210 (2021) 365–376.
- [20] P.R. Yaashikaa, P.S. Kumar, A. Saravanan, D.-V.N. Vo, Advances in biosorbents for removal of environmental pollutants: a review on pretreatment, removal mechanism and future outlook, *J. Hazard. Mater.*, 420 (2021) 126596, doi: 10.1016/j.jhazmat.2021.126596.
- [21] A. Saravanan, P. Senthil Kumar, B. Preetha, Optimization of process parameters for the removal of chromium(VI) and nickel(II) from aqueous solutions by mixed biosorbents (custard apple seeds and *Aspergillus niger*) using response surface methodology, *Desal. Water Treat.*, 57 (2016) 14530–14543.
- [22] A. Saravanan, S. Karishma, P.S. Kumar, S. Varjani, P.R. Yaashikaa, S. Jeevanantham, R. Ramamurthy, B. Reshma, Simultaneous removal of Cu(II) and reactive green 6 dye from wastewater using immobilized mixed fungal biomass and

- its recovery, *Chemosphere*, 271 (2021) 129519, doi: 10.1016/j.chemosphere.2020.129519.
- [23] A. Saravanan, P.S. Kumar, P.R. Yaashikaa, S. Karishma, S. Jeevanantham, S. Swetha, Mixed biosorbent of agro waste and bacterial biomass for the separation of Pb(II) ions from water system, *Chemosphere*, 277 (2021) 130236, doi: 10.1016/j.chemosphere.2021.130236.
- [24] A. Saravanan, T.R. Sundararaman, S. Jeevanantham, S. Karishma, P.S. Kumar, P.R. Yaashikaa, Effective adsorption of Cu(II) ions on sustainable adsorbent derived from mixed biomass (*Aspergillus campestris* and agro waste): optimization, isotherm and kinetics study, *Groundwater Sustainable Dev.*, 11 (2020) 100460, doi: 10.1016/j.gsd.2020.100460.
- [25] R. Jain, P. Sharma, S. Sikarwar, J. Mittal, D. Pathak, Adsorption kinetics and thermodynamics of hazardous dye Tropaeoline 000 onto Aeroxide Alu C (nano alumina): a non-carbon adsorbent, *Desal. Water Treat.*, 52 (2014) 7776–7783.
- [26] Y.S. Ren, H. Khan, B. Khan, M. Ilyas, S. Iqbal, Application of eucalyptus wood waste derived biochar for adsorption of aluminum from aqueous solutions, *Desal. Water Treat.*, 287 (2023) 116–123.
- [27] M. Ilyas, W. Ahmad, H. Khan, Polycyclic aromatic hydrocarbons removal from vehicle-wash wastewater using activated char, *Desal. Water Treat.*, 236 (2021) 55–68.
- [28] M. Ilyas, H. Khan, W. Ahmad, Conversion of waste plastics into carbonaceous adsorbents and their application for wastewater treatment, *Int. J. Environ. Anal. Chem.*, (2022), doi: 10.1080/03067319.2022.2062571.
- [29] J.L. Figueiredo, J.A. Moulijn, *Carbon and Coal Gasification: Science and Technology*, Vol. 105, Springer Dordrecht, 2012.
- [30] S. Wadhawan, A. Jain, J. Nayyar, S.K. Mehta, Role of nanomaterials as adsorbents in heavy metal ion removal from wastewater: a review, *J. Water Process Eng.*, 33 (2020) 101038, doi: 10.1016/j.jwpe.2019.101038.
- [31] V.K. Gupta, I. Ali, T.A. Saleh, M.N. Siddiqui, S. Agarwal, Chromium removal from water by activated carbon developed from waste rubber tires, *Environ. Sci. Pollut. Res.*, 20 (2013) 1261–1268.
- [32] J. Lyklema, *Fundamentals of Interface and Colloid Science*, Vol. II. Solid–Liquid Interfaces, Academic Press, New York, 1995.
- [33] A. Puzskarewicz, J. Kaleta, The efficiency of the removal of naphthalene from aqueous solutions by different adsorbents, *Int. J. Environ. Res. Public Health*, 17 (2020) 5969, doi: 10.3390/ijerph17165969.
- [34] M. Smol, M. Włodarczyk-Makuła, M.D. Włóka, Adsorption of polycyclic aromatic hydrocarbons (PAHs) from aqueous solutions on different sorbents, *Civ. Environ. Eng. Rep.*, 13 (2014) 87–96.
- [35] A. Awoyemi, *Understanding the Adsorption of Polycyclic Aromatic Hydrocarbons From Aqueous Phase onto Activated Carbon*, University of Toronto, Toronto (ON), 2011.
- [36] M. Yuan, S. Tong, S. Zhao, C.Q. Jia, Adsorption of polycyclic aromatic hydrocarbons from water using petroleum coke-derived porous carbon, *J. Hazard. Mater.*, 181 (2010) 1115–1120.